SUPPLEMENTARY APPENDIX

Coactosin-like 1 integrates signaling critical for shear-dependent thrombus formation in mouse platelets

Inga Scheller,[1,2] Simon Stritt,[1,2,°] Sarah Beck,[1,2] Bing Peng,[3] Irina Pleines,[1,2] Katrin G. Heinze,[2] Attila Braun,[1,2] Oliver Otto,[4] Robert Ahrends,[3] Albert Sickmann,[3] Markus Bender,[1,2] and Bernhard Nieswandt[1,2]

[1]Institute of Experimental Biomedicine I, University Hospital, University of Würzburg, Würzburg; [2]Rudolf Virchow Center, University of Würzburg, Würzburg; [3]Leibniz-Institut für Analytische Wissenschaften - ISAS – e.V., Lipidomics, Dortmund and [4]Center for Innovation Competence - Humoral Immune Reactions in Cardiovascular Diseases, Biomechanics, University of Greifswald, Greifswald, Germany.

°Current affiliation: Department of Immunology, Genetics and Pathology, Uppsala University, Uppsala, Sweden.

 doi:10.3324/haematol.2019.225516

Received: April 29, 2019.

Accepted: September 26, 2019.

Pre-published: October 3, 2019.

Correspondence: *BERNHARD NIESWANDT* - bernhard.nieswandt@virchow.uni-wuerzburg.de

Coactosin-like 1 integrates signaling critical for shear-dependent thrombus formation in mouse platelets

Inga Scheller[1,2], Simon Stritt[1,2,#], Sarah Beck[1,2], Bing Peng[3], Irina Pleines[1,2], Katrin G. Heinze[2], Attila Braun[1,2], Oliver Otto[4], Robert Ahrends[3], Albert Sickmann[3], Markus Bender[1,2], and Bernhard Nieswandt[1,2,*]

[1]Institute of Experimental Biomedicine I, University Hospital, University of Würzburg, Würzburg, Germany.

[2]Rudolf Virchow Center, University of Würzburg, Würzburg, Germany.

[3]Leibniz-Institut für Analytische Wissenschaften - ISAS – e.V., Lipidomics, Dortmund, Germany.

[4]Centre for Innovation Competence - Humoral Immune Reactions in Cardiovascular Diseases, Biomechanics, University of Greifswald, Greifswald, Germany.

[#]Current affiliation: Department of Immunology, Genetics and Pathology, Uppsala University, Uppsala, Sweden.

Running head: Cotl1 regulates shear-dependent thrombus formation

SUPPLEMENTAL METHODS

Platelet preparation

Mice were bled under isoflurane anesthesia into heparin (20 U mL^{-1}, Ratiopharm) and blood was centrifuged twice for 6 minutes at 300 g. Platelet-rich plasma (PRP) was supplemented with 2 µL mL^{-1} apyrase (0.02 U mL^{-1}; A6410, Sigma-Aldrich) and 5 µL mL^{-1} PGI_2 (0.1 µg mL^{-1}; P6188, Sigma-Aldrich) and platelets were pelleted by centrifugation for 5 minutes at 800 g, washed twice with Tyrode-HEPES buffer (134 mM NaCl, 0.34 mM Na_2HPO_4, 2.9 mM KCl, 12 mM $NaHCO_3$, 5 mM HEPES, 5 mM glucose, 0.35% BSA, pH 7.4) containing 2 µL mL^{-1} apyrase and 5 µL mL^{-1} PGI_2 and allowed to rest for 30 minutes prior to experiments.

Flow cytometry

50 µL of blood were withdrawn under isoflurane anesthesia, washed twice with Tyrode-HEPES buffer and finally diluted (1:20) in Tyrode-HEPES buffer containing 2 mM Ca^{2+}. Samples (washed blood) were activated with the indicated agonists. Activation of αIIbβ3- (JON/A-PE, Emfret) (1) and P-selectin exposure (WUG.E9-FITC) were determined using fluorophore-conjugated antibodies (15 minutes at 37°C). Analysis was performed on a FACSCalibur (BD Biosciences) (2).

Aggregometry

Light transmission of washed platelets (1.5 x 10^5 platelets per µL) supplemented with 100 µg mL^{-1} fibrinogen (Sigma-Aldrich) was monitored over time using a four-channel aggregometer (APACT, Laborgeräte und Analysensysteme, Hamburg). Platelet aggregation was induced by addition of the indicated agonists.

Platelet adhesion under flow

Mice were bled under isoflurane anesthesia into heparin (20 U mL^{-1}, Ratiopharm). Anticoagulated whole blood was perfused over collagen I-coated cover slips (100 µg mL^{-1} Horm collagen, Nycomed) at a shear rate of 150, 1 000, 1 700 and 3 000 s^{-1}. Prior to perfusion, platelets were labeled with a Dylight-488-conjugated anti-GPIX derivative (0.2 µg mL^{-1}) for 5 minutes at 37°C. Phase-contrast and fluorescence images were recorded with a Zeiss Axiovert 200 inverted microscope (40x/0.60 objective) equipped with a CoolSNAP-EZ camera (Visitron) and analyzed off-line using Metavue software.

Coagulation flow chamber

Mice were bled under isoflurane anesthesia into sodium citrate (0.129 M). Collagen-coated and BSA-blocked coverslips were perfused with citrated blood, which was recalcified with Tyrode´s-HEPES buffer supplemented with 63 mM $CaCl_2$ and 32 mM $MgCl_2$ by co-infusion in a 1:10 ratio via a Y-shaped dual inlet tube at a shear rate of 1 000 s^{-1}. Prior to perfusion, blood samples were pre-labeled with Alexa Fluor 488-labeled fibrinogen and an Alexa Fluor 647-labeled anti-GPIX derivative for 5 min at 37°C. Blood was perfused for 6 min and afterwards coverslips were washed for another 6 min. At the end of the perfusion time, phase-contrast and fluorescence images were recorded with a Zeiss Axiovert 200 inverted microscope (40x/0.60 objective) equipped with a CoolSNAP-EZ camera (Visitron) and analyzed off-line using Metavue software.

Tail bleeding time

Tail bleeding assays were performed as described (3). Mice were anesthetized and a 2 mm segment of the tail tip was removed using a scalpel. Tail bleeding was monitored by gently absorbing blood on a filter paper at 20 s intervals without making contact with the wound site. Bleeding was determined to have ceased when no blood was observed on the paper. Experiments were stopped after 20 minutes by cauterization. Differences between the mean bleeding time was statistically assessed using the Student's t-test and differences between occluded and non-occluded vessels by Fisher's t-test.

Aorta injury model

The abdominal cavity of anesthetized mice was opened to expose the abdominal aorta. An ultrasonic flow probe (0.5PSB699; Transonic Systems, USA) was placed around the abdominal aorta, and thrombus formation was induced by a single firm compression with forceps upstream of the flow probe. Blood flow was monitored for 30 minutes or until vessel occlusion occurred (blood flow stopped for > 5 minutes). Differences between occluded and non-occluded vessels were statistically assessed using the Fisher's t-test.

F-actin assembly

F-actin polymerization has been described previously (4). Washed platelets were incubated with a DyLight-649-labeled anti-GPIX antibody derivative (20 µg mL^{-1}) and either remained resting or were stimulated with the indicated agonists for 2 min. The cells were fixed with 55 % of total volume of 10% paraformaldehyde in PHEM buffer, centrifuged and resuspended in 55 µL of Tyrode's buffer supplied with Ca^{2+} and 0.1% Triton™ X100. Subsequently, platelets were stained with 10 µM phalloidin-FITC (P5282, Sigma-Aldrich) for 30 min and immediately analyzed on a FACSCalibur.

Immunostaining of spread platelets

Spreading and immunostaining of platelets were performed as described previously (5). Briefly, coverslips were coated with fibrinogen (100 µg mL^{-1}; F4883, Sigma-Aldrich) overnight at 4°C. Washed platelets were stimulated with 0.01 U mL^{-1} thrombin (10602400001, Roche) and allowed to spread. At the indicated time points, platelets were fixed and permeabilized in PHEM buffer supplemented with 4% para-formaldehyde (PFA) and 1% IGEPAL® CA-630 and stained with phalloidin-Atto647N (170 nM, 65906, Fluka) and anti-α-tubulin Alexa F488 (3.33 µg mL-1, 322588 (B-5-1-2), Invitrogen). Samples were mounted with Fluoroshield (F6182, Sigma-Aldrich) and images acquired using a Leica TCS SP5 confocal microscope (Leica Microsystems).

TxB_2 ELISA

Washed platelets were either left untreated or stimulated with CRP (5 and 1 µg mL^{-1}) or thrombin (0.01 and 0.001 U mL^{-1}) for 5 min. The reaction was stopped by adding 5 mM EDTA and 1 mM aspirin. Platelets were removed by centrifugation at 14 000 rpm for 5 min and the supernatant was collected. TxB_2 concentrations in the supernatant were measured using the TxB_2 ELISA kit according to the manufacturer's instructions (DRG, Marburg, Germany).

Transmission electron microscopy

To visualize platelet ultrastructure, platelet-rich plasma was prepared and platelets were fixed with 2.5% glutaraldehyde (16210, Electron Microscopy Sciences) in 50 mM cacodylate buffer (pH 7.2; 12201, AppliChem). Platelets were embedded in epon 812 (14900, Electron Microscopy Sciences), ultrathin sections were generated and stained with 2% uranyl acetate (22400, Electron Microscopy Sciences) and lead citrate (17800, Electron Microscopy Sciences). The visualization of the cytoskeleton of resting and spread platelets was performed as previously described (6). Images were acquired on an EM900 electron microscope (Carl Zeiss).

Immunoblotting

Denatured or native lysates of resting and activated platelets were separated by SDS-PAGE and blotted onto PVDF membranes. GAPDH (1 µg mL-1, G5262, Sigma-Aldrich), Twf1 (1 µg mL-1), Twf2a (1 µg mL-1), full length (#3311, Cell Signaling) and phosphorylated n-cofilin (#5175, Cell Signaling) were probed with the respective antibodies and detected using horseradish peroxidase-conjugated secondary antibodies (0.33 µg ml^{-1}) and enhanced chemiluminescence solution (JM-K820-500, MoBiTec). Images were recorded using a MultiImage® II FC Light Cabinet (Alpha Innotech cooperation) device. Anti-Twf1 and -Twf2 antibodies were a kind gift from Pekka Lappalainen (Helsinki, Finland).

Real-time deformability cytometry

RT-DC measurements of platelets were performed as described by Otto *et al.* (7). Briefly, whole blood was collected into EDTA-microvettes (Sarstedt). Afterwards, the mechanical properties of several thousands of platelets were calculated from shear-induced deformations inside a 300 μm long constriction of 15 μm x 15 μm cross-section. This microfluidic system is assembled on the commercial AcCellerator system (Zellmechanik Dresden) consisting of an inverted microscope, a pulsed 2 μs brightfield illumination and a syringe pump driving the cell suspension through the constriction. Measurements were performed at flow rates of 6 nL s^{-1} using heparinized peripheral blood diluted 1:20 in PBS (with 0.6% (w/v) methylcellulose) and a size gate was applied to analyze exclusively platelets, only. For reference a measurement was taken in the reservoir of the microfluidic chip before cells were exposed to mechanical stress. Deformation was calculated from the circularity of each cell:

$$Deformation = 1 - circularity = 1 - \frac{2\sqrt{\pi Area}}{Perimeter} \quad ,$$

where the area and perimeter are calculated in real-time using ShapeIn software (Zellmechanik Dresden) for up to 1,000 cells per second from the brightfield images. Data analysis was performed using three experimental replicates where statistical significance was calculated based on linear mixed models and using ShapeOut software (Zellmechanik Dresden) (8). Before starting a measurement and between experimental replicates the entire fluidic system was flushed with 70% ethanol and de-ionized water. Flow was equilibrated for 2 min between samples.

Lipid mediator extraction and analysis

Lipid mediator extraction and analysis of platelets were performed as described by Peng *et al.* (9). In summary, washed platelets were either left untreated or stimulated with 1 U mL^{-1} thrombin (Sigma) or 5 μg mL^{-1} CRP for 5 min at 37°C. After centrifugation for 5 min at 300 g, the pellet and supernatant were separated and shock frozen in liquid nitrogen and lipid extraction was performed as follows: 225 µL of MeOH (4 °C) were added to the platelet cell pellet or supernatant in an Eppendorf polypropylene tube that was placed on ice. After a few seconds of treatment with ultrasonication and vortexing, 10 µL of the internal standard mixture (5 mg L^{-1} of 12-HETE-d8, 5-HETE-d8, 5-OxoETE-d7 and AA-d8; 0.5 mg L^{-1} of PGE2-d9 and TXB2-d4; 0.2 mg L^{-1} of LTB4-d4, LTC4-d5 and LTD4-d5; and 0.25 mg L^{-1} of DHA-d5), 20 µL of acetic acid (99.99%, 17.5 M) and 750 µL of MTBE (4 °C) were added. The mixture was incubated for 1 h at 4 °C in a thermomixer at 650 rpm. Subsequently, 235 µL (for pellet) or 188 µL (for supernatant) of ultrapure water was added to induce phase separation. The samples were centrifuged at 10 000 g for 10 min at 4 °C, afterwards the upper organic layer

was transferred to another Eppendorf tube and dried under continuous N_2 flow. The dried lipid extract was resuspended in 50 µL of MeOH for further MS analysis. The lower layer of pellet extraction was used to precipitate proteins by adding 1220 µL MeOH after removing the interphase and samples were stored at -80 °C for 3 h in order to perform protein precipitation. Protein pellets were collected after centrifugation at 19 000 g for 30 min at 4 °C and stored in 1 % SDS, 150 mM NaCl, 50 mM Tris (pH 7.8) solution at -80 °C. Protein amount was quantified by BCA (bicinchoninic acid assay, Thermo Fisher Scientific, Rockford, USA).

For the reverse-phase liquid chromatography (LC), an UltiMate 3000-system from Thermo Fischer Scientific (Darmstadt, Germany) was employed. The chromatographic separation was performed on an Ascentis Express C18 main column (150 mm × 2.1 mm, 2.7 µm, Supelco) fitted with a guard cartridge (50 mm × 2.1 mm, 2.7 µm, Supelco). The temperatures of the autosampler and the column oven were set at 10 °C and 30 °C, respectively. Solvent A was ACN/H_2O (3:7, v/v) and 0.1 % formic acid while solvent B was IPA/ACN (1:1, v/v). The separation was carried out at a flow rate of 0.4 mL min^{-1} with the following 20 min long gradient: initial (0 % B), 0.0-1.0 min (hold 0 % B), 1.0-13.0 min (0-100 % B), 13.0-16.0 min (hold 100 % B), 16.0 min (0 % B), 16.0-20.0 min (hold 0 % B). Solvent A was also used as transfer solution for injection. Samples and standards were injected with a volume of 5 µL and analyzed in triplicates, respectively. The LC was coupled to a QTRAP 6500 (Applied Biosystems, Darmstadt, Germany) which was equipped with an electrospray ion source (Turbo V Ion Source). The following ESI source settings were used for negative mode: curtain gas 10 arbitrary units, temperature 525 °C, ion source gas I 30 arbitrary units, ion source gas II 55 arbitrary units, collision gas medium; ion spray voltage -4500 V, entrance potential -10 V, and exit potential 10 V. In multiple reaction monitoring (MRM), at least two fragments per lipid were added into the transition list. Skyline (64-bit, 4.1.0.11796) was used to visualize results, integrate signals, and quantify all lipids that were detected by MS.

Data analysis

The presented results are mean ± standard deviation (S.D.) from at least three independent experiments, if not stated otherwise. Unless stated otherwise, data distribution was analyzed using the Shapiro-Wilk-test and differences between *WT* and *Cotl1*$^{-/-}$ mice were statistically analyzed using Student's-t- or Wilcoxon-Mann-Whitney-test (SigmaPlot, Systat Software Inc., Version 14.0). Differences between more than two groups were statistically analyzed using ANOVA + post hoc test for multiple comparisons. *P*-values < 0.05 were considered as statistically significant **P*< 0.05; ***P*< 0.01; ****P*< 0.001.

SUPPLEMENTAL REFERENCES

1. Bergmeier W, Schulte V, Brockhoff G, Bier U, Zirngibl H, Nieswandt B. Flow cytometric detection of activated mouse integrin αIIbβ3 with a novel monoclonal antibody. Cytometry. 2002;48(2):80-86.
2. Stritt S, Wolf K, Lorenz V, et al. Rap1-GTP-interacting adaptor molecule (RIAM) is dispensable for platelet integrin activation and function in mice. Blood. 2015;125(2):219-222.
3. Stritt S, Birkholz I, Beck S, et al. Profilin 1–mediated cytoskeletal rearrangements regulate integrin function in mouse platelets. Blood Advances. 2018;2(9):1040-1045.
4. Stritt S, Beck S, Becker IC, et al. Twinfilin 2a regulates platelet reactivity and turnover in mice. Blood. 2017;130(15):1746-1756.
5. Bender M, Stritt S, Nurden P, et al. Megakaryocyte-specific Profilin1-deficiency alters microtubule stability and causes a Wiskott-Aldrich syndrome-like platelet defect. Nat Commun. 2014;5(4746.
6. Spindler M, van Eeuwijk JMM, Schurr Y, et al. ADAP deficiency impairs megakaryocyte polarization with ectopic proplatelet release and causes microthrombocytopenia. Blood. 2018;blood-2018-2001-829259.
7. Otto O, Rosendahl P, Mietke A, et al. Real-time deformability cytometry: on-the-fly cell mechanical phenotyping. Nature Methods. 2015;12(199.
8. Herbig M, Mietke A, Müller P, Otto O. Statistics for real-time deformability cytometry: Clustering, dimensionality reduction, and significance testing. Biomicrofluidics. 2018;12(4):042214.
9. Peng B, Geue S, Coman C, et al. Identification of key lipids critical for platelet activation by comprehensive analysis of the platelet lipidome. Blood. 2018;
10. Samuelsson B. Leukotrienes: mediators of immediate hypersensitivity reactions and inflammation. Science. 1983;220(4597):568-575.
11. Samuelsson B, Dahlen S, Lindgren J, Rouzer C, Serhan C. Leukotrienes and lipoxins: structures, biosynthesis, and biological effects. Science. 1987;237(4819):1171-1176.

SUPPLEMENTAL TABLE

Supplemental Table 1. Platelet surface glycoprotein expression in *Cotl1*$^{-/-}$ platelets. Diluted whole blood was stained with fluorophore-labeled antibodies and analyzed on a FACSCalibur (Becton Dickinson, Heidelberg). Platelets were gated by FSC/SSC characteristics. Results are given as the MFI ± S.D. of 12 mice per group.

	WT	***Cotl1*$^{-/-}$**
GPIb	268±36	294±16
GPV	213±4	222±5
GPIX	384±10	396±10
CD9	668±20	661±21
GPVI	36±2	36±2
CLEC-2	110±6	113±5
Integrin α2	43±4	45±3
Integrin β1	131±2	136±4
Integrin αIIbβ3	438±31	425±21

SUPPLEMENTAL FIGURES & LEGENDS

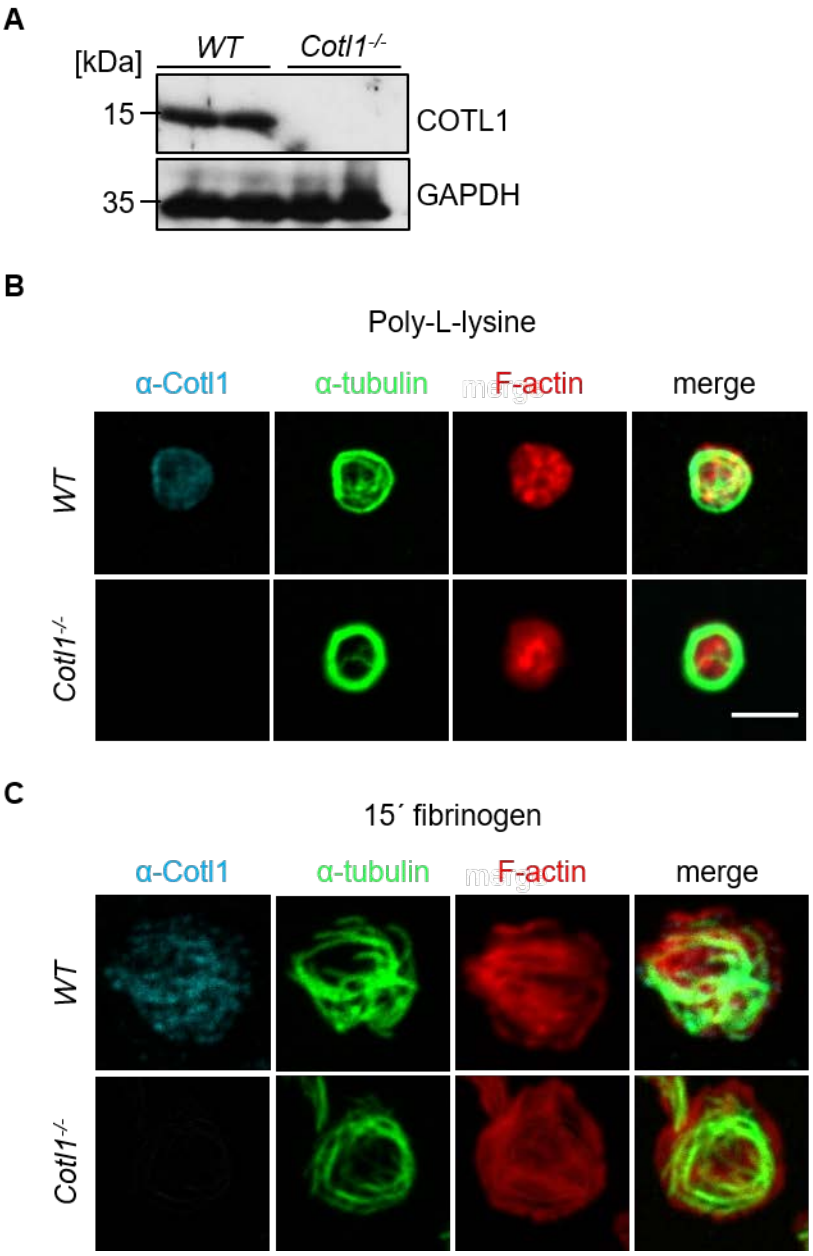

Supplemental Figure 1. Cytoplasmic localization of Cotl1. (**A**) Immunoblot on platelet lysates proved the complete loss of Cotl1 in mutant platelets. GAPDH served as loading control. (**B, C**) Localization of Cotl1 in resting and spread platelets was assessed by confocal imaging of resting and spread (15 min) platelets on fibrinogen (100 µg mL^{-1}), which were immunostained for F-actin (red), α-tubulin (green) and α-Cotl1 (cyan). Scale bars, 3 µm. Images were acquired with a TCS SP8 confocal microscope (100x/1.4 oil STED WHITE objective, Leica Microsystems) and are representative of at least 10 individuals per group.

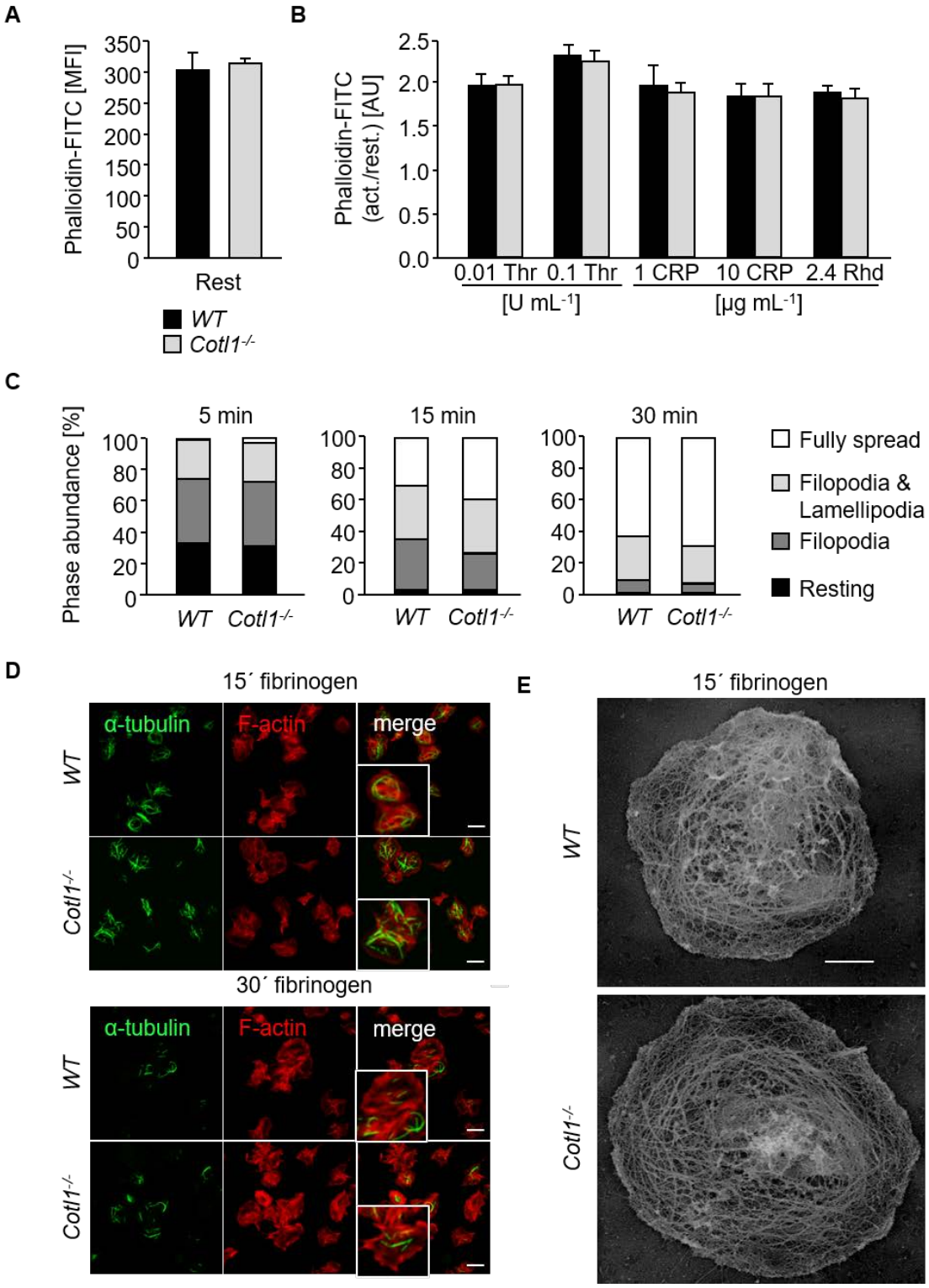

Supplemental Figure 2. Cotl1 is dispensable for actin dynamics in platelets. (**A, B**) Relative F-actin content of resting and activated platelets was determined by flow cytometry. Values are mean ± S.D. of 4 mice per group. The values shown are the ratio of MFI from activated and resting platelets. (**C**) Washed platelets were allowed to spread (15 min) on fibrinogen (100 µg mL^{-1}) and phase abundance was determined. (**D**) Confocal fluorescence

microscopy images of spread platelets (15 and 30 min) on fibrinogen (100 µg mL^{-1}) immunostained for F-actin (red) and α-tubulin (green). Scale bar, 3 µm. Images were acquired with a TCS SP8 confocal microscope (100x/1.4 oil STED WHITE objective, Leica Microsystems) and are representative of at least 10 individuals per group. (**E**) Representative images of the platelet cytoskeleton ultrastructure on fibrinogen (15 min). Scale bar, 1 µm.

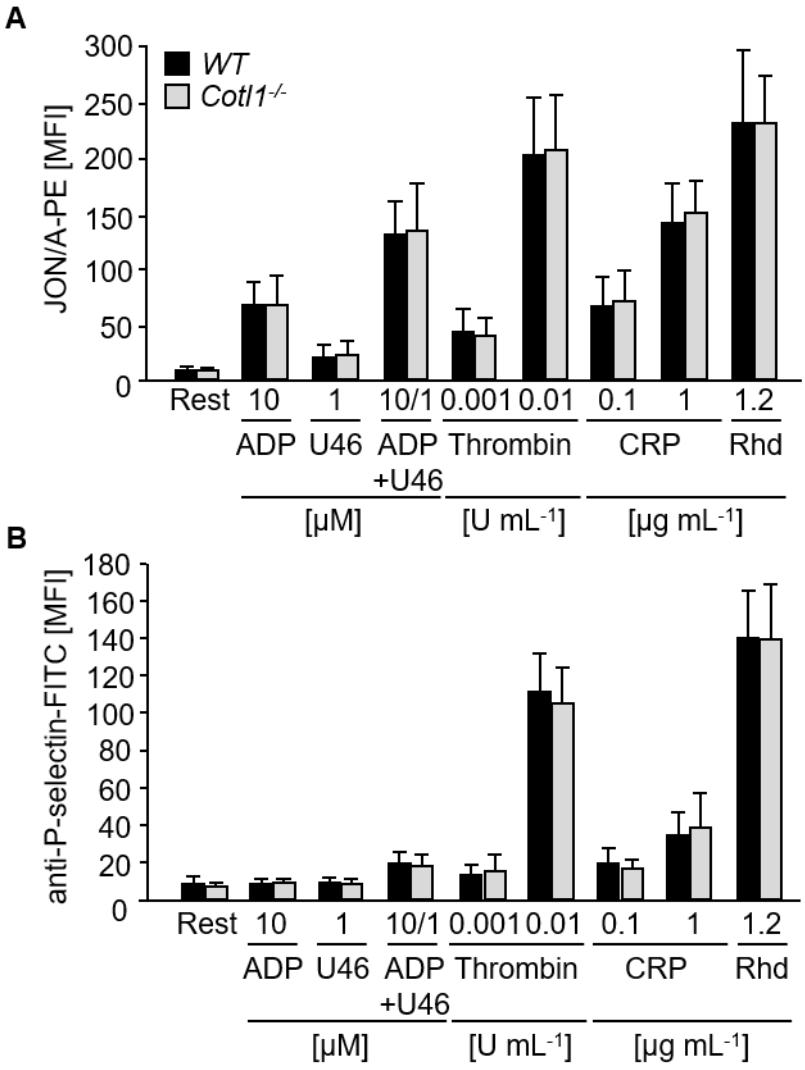

Supplemental Figure 3. Unaltered activation in Cotl1-deficient platelets under static conditions *in vitro*. (**A, B**) Activation of platelet αIIbβ3 integrin (JON/A-PE) (**A**) and degranulation (α-P-selectin-FITC) (**B**) in *Cotl1*$^{-/-}$ platelets upon stimulation with the indicated agonists was determined by flow cytometry (n = 12). U46, U46619; CRP, collagen-related peptide; Rhd, rhodocytin

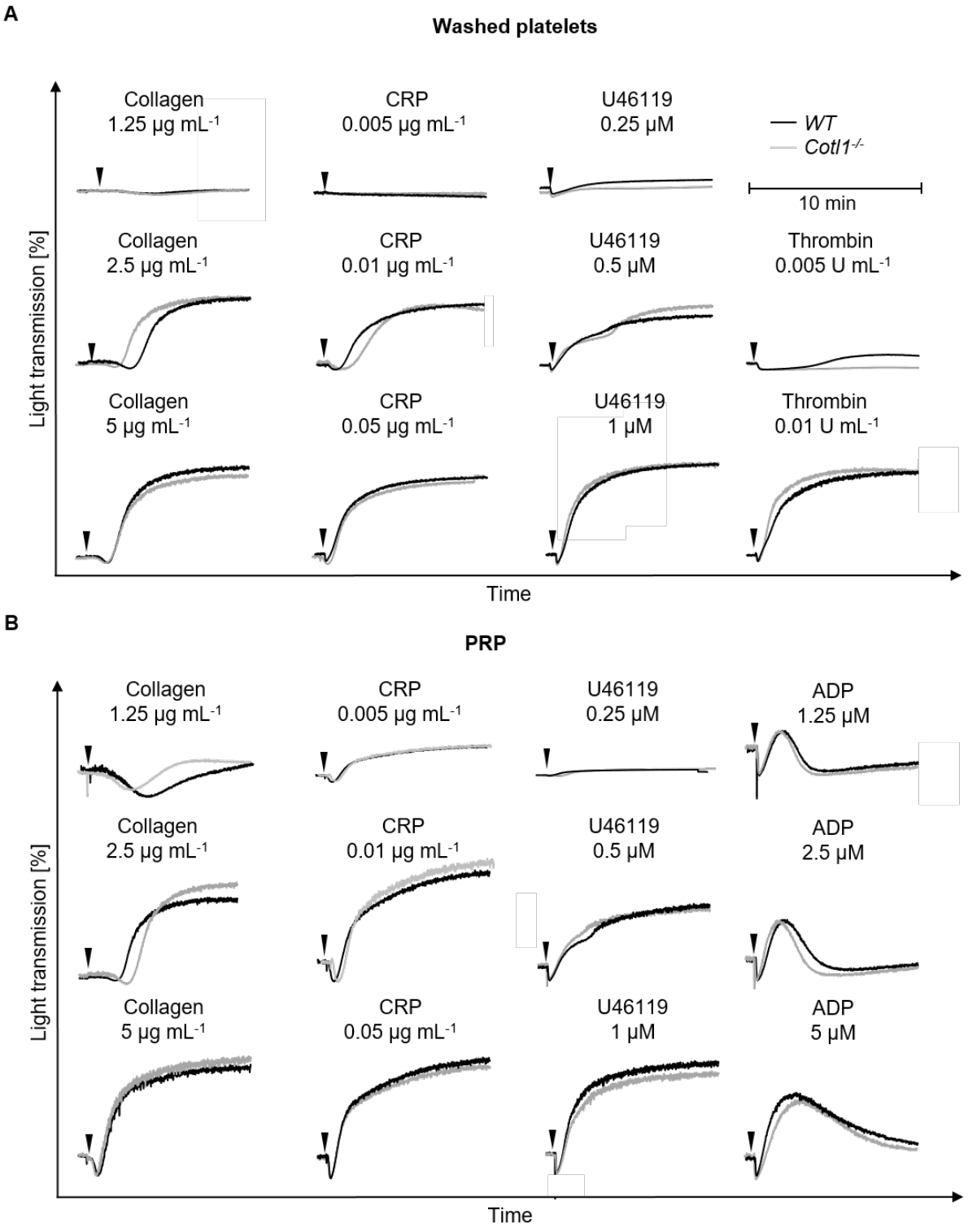

Supplemental Figure 4. Unaltered platelet aggregation in Cotl1-deficient platelets. (**A**) Aggregation responses of washed platelets (**A**) and platelet-rich plasma (PRP) (**B**) in turbidometric aggregometry after stimulation with the indicated agonists (n = 6). The arrow indicates addition of the agonist.

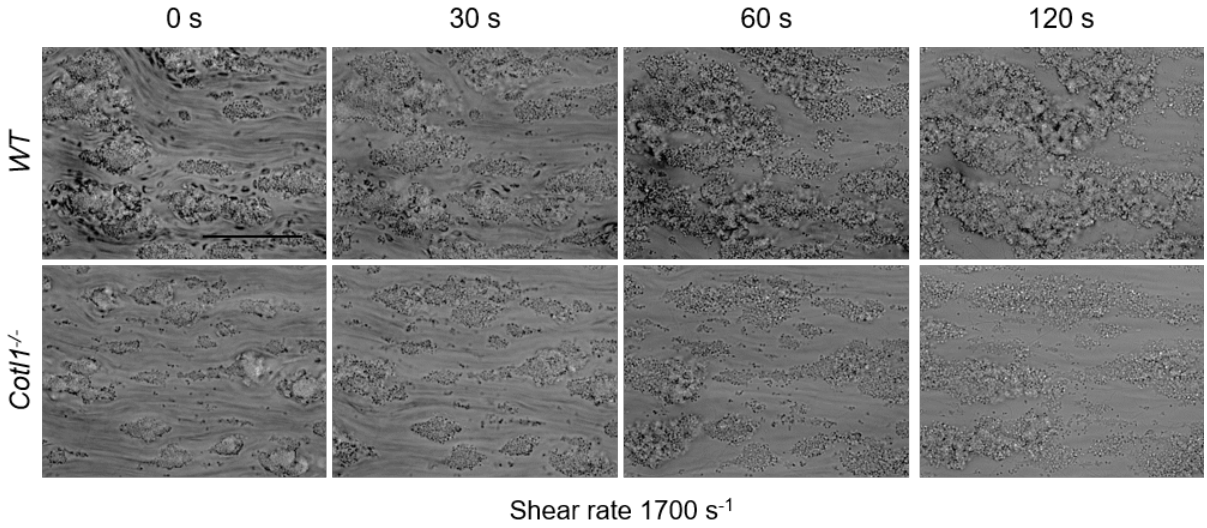

Supplemental Figure 5. Impaired adhesion and thrombus formation of *Cotl1*$^{-/-}$ platelets on collagen under flow. Heparinized whole blood of *WT* and *Cotl1*$^{-/-}$ mice was perfused over a collagen I-coated surface for 4 min at a shear rate of 1,700 s^{-1}. Representative brightfield images were acquired at the indicated time points during the perfusion period. Values are mean ± S.D. (n = 12). Scale bar, 50 µm.

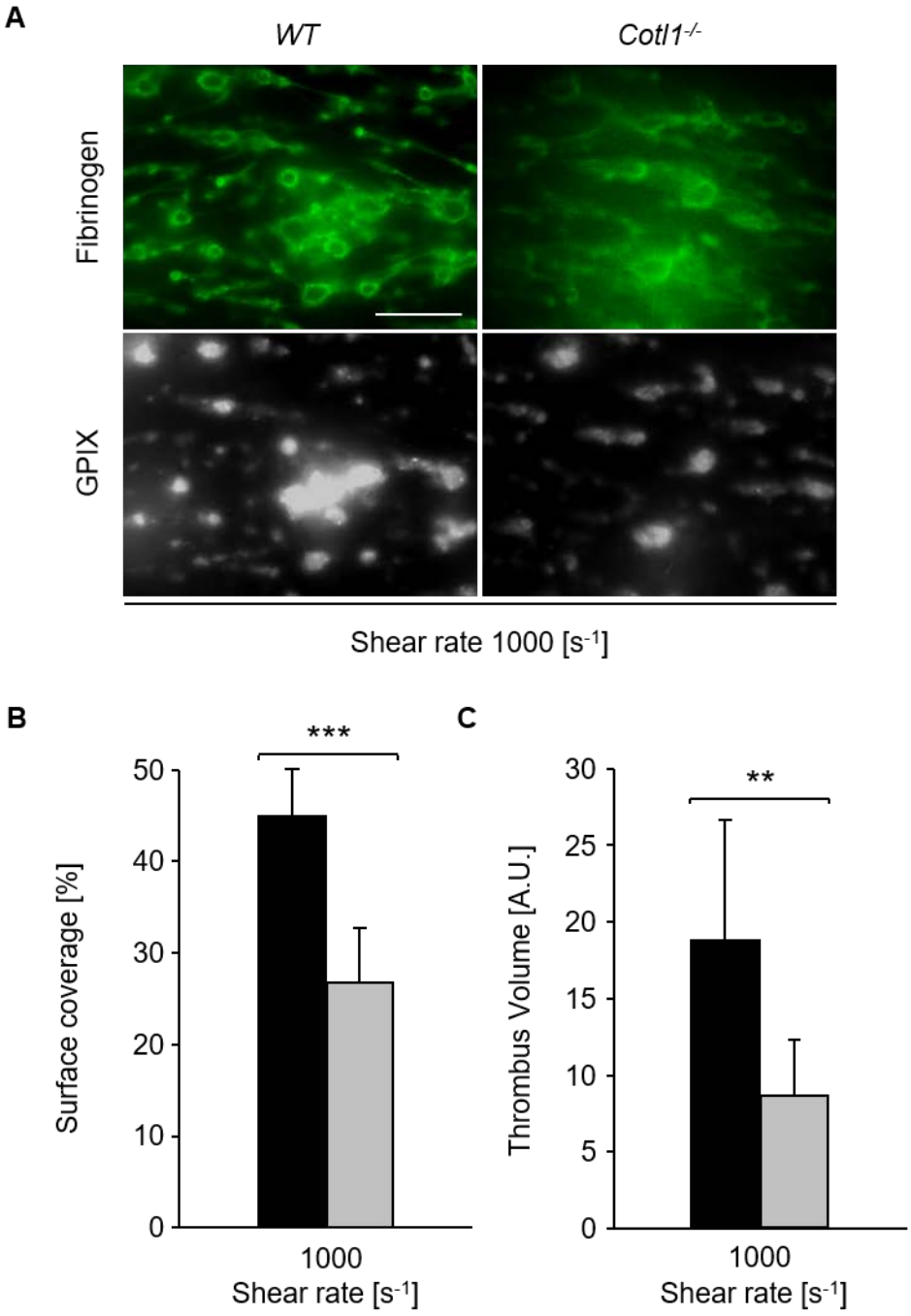

Supplemental Figure 6. Reduced aggregate formation of *Cotl1*$^{-/-}$ platelets under flow in the presence of coagulation. Assessment of platelet adhesion (**A, B**) and aggregate formation (**A, C**) on Horm collagen (70 µg mL^{-1}) under flow (1000 s^{-1}). Collagen-coated coverslips were perfused with citrated blood, which was recalcified with Tyrode´s-HEPES buffer supplemented with 63 mM $CaCl_2$ and 32 mM $MgCl_2$. Before each experiment, blood samples from *WT* and *Cotl1*$^{-/-}$ mice were pre-labeled with Alexa Fluor 488-labeled fibrinogen and an Alexa Fluor 647-labeled anti-GPIX antibody. Values are mean ± S.D. (n = 9). Scale bar, 50 µm.

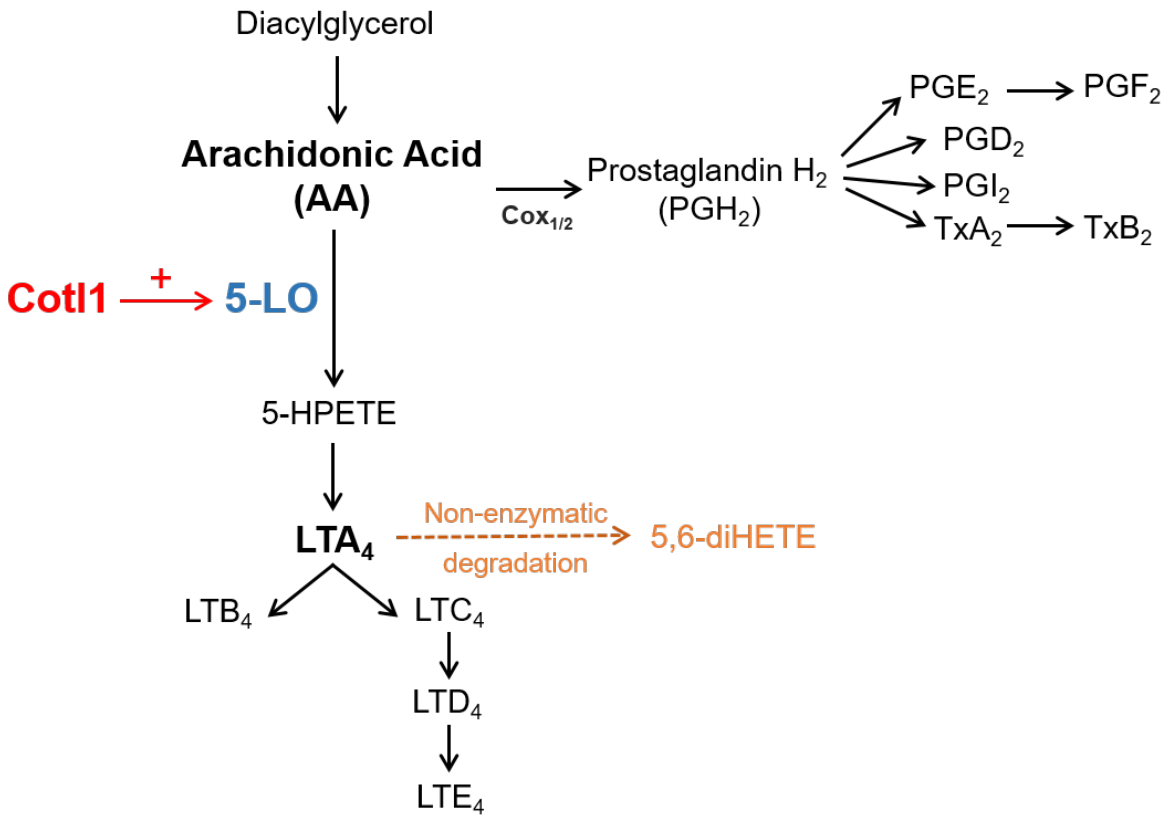

5-LO: 5-lipoxygenase
Cox: Cyclooxygenase
5-HPETE: 5(S)hydroperoxy-6-trans-8,11,14-cis-eicosatetraenoic acid
LT: Leukotriene
TxA_2: Thromboxane A_2
5,6-diHETE: 5,6-dihydroxy-8Z,11Z,14Z,17Z-eicosatetraenoic acid

Supplemental Figure 7. The 5-LO pathway. 5-LO catalyzes the two initial steps of LT biosynthesis, (1) the oxygenation of AA to 5-HPETE and (2) the subsequent dehydration into the epoxide LTA_4 (10, 11). Likewise, 5-HPETE can be reduced to 5-HETE, which is metabolized to 5-oxo-ETE. AA is also converted to thromboxanes (TxA/B_2), prostacyclin (PGI_2) and prostaglandines (PGE/F_2) by cyclooxygenases (Cox).

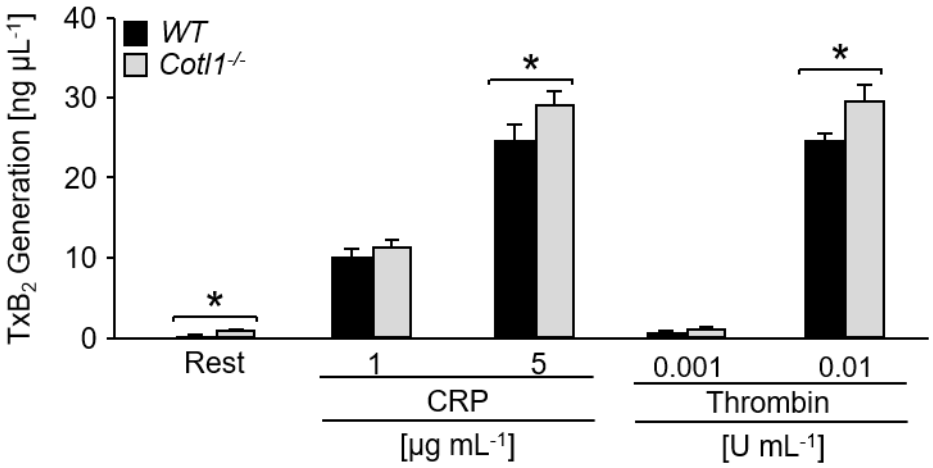

Supplemental Figure 8. Increased thromboxane B_2 production in *Cotl1*$^{-/-}$ platelets. TxB_2 levels were measured in the supernatant of resting and stimulated washed platelets by ELISA. Results are expressed as mean TxB_2 generation [ng mL^{-1}] ± S.D. of 6 mice per group. *P< 0.05.

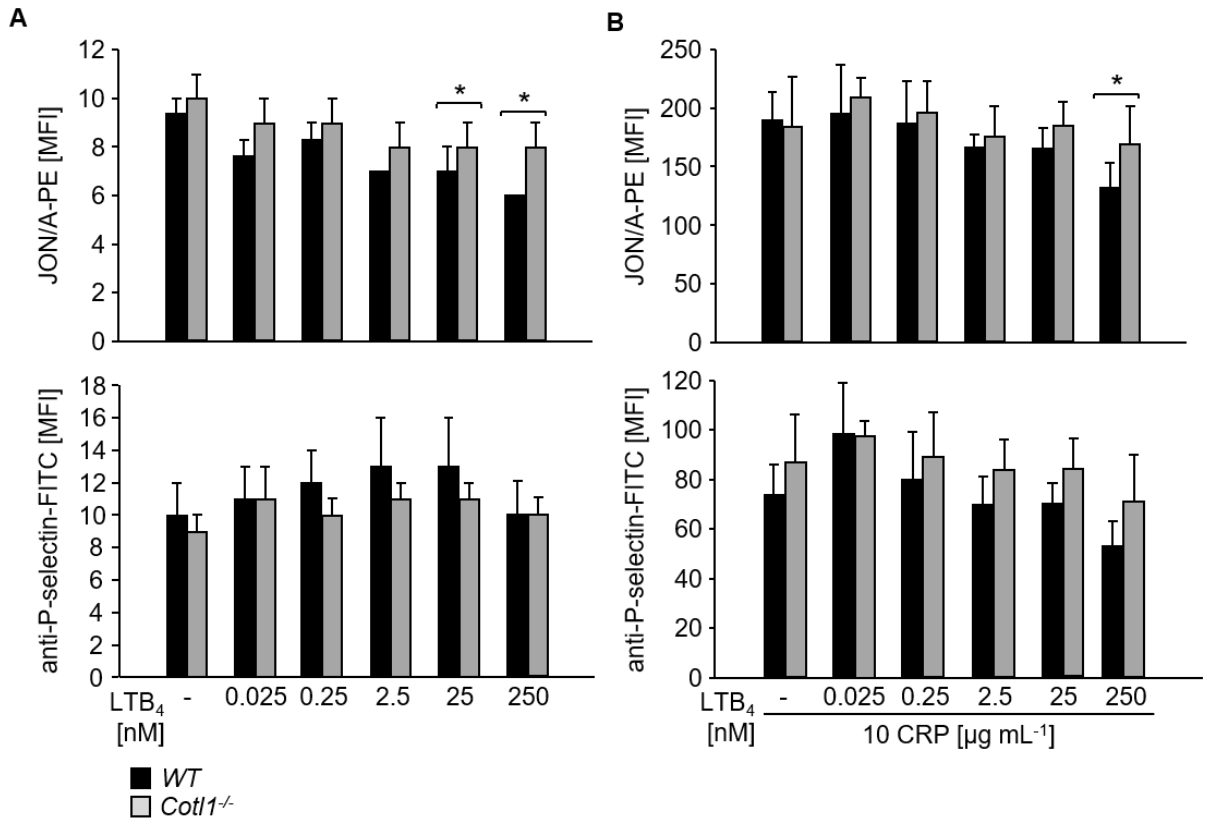

Supplemental Figure 9. LTB_4 treatment does not induce platelet activation under static conditions. (**A- C**) Assessment of platelet αIIbβ3 integrin (JON/A-PE) activation and degranulation (α-P-selectin-FITC) in *WT* and *Cotl1*$^{-/-}$ platelets by flow cytometry. Platelets were stimulated with (**A**) 250-0.025 nM LTB_4 or (**B**) co-stimulated with 10 µg mL^{-1} CRP. *P< 0.05; **P< 0.01; ***P< 0.001.

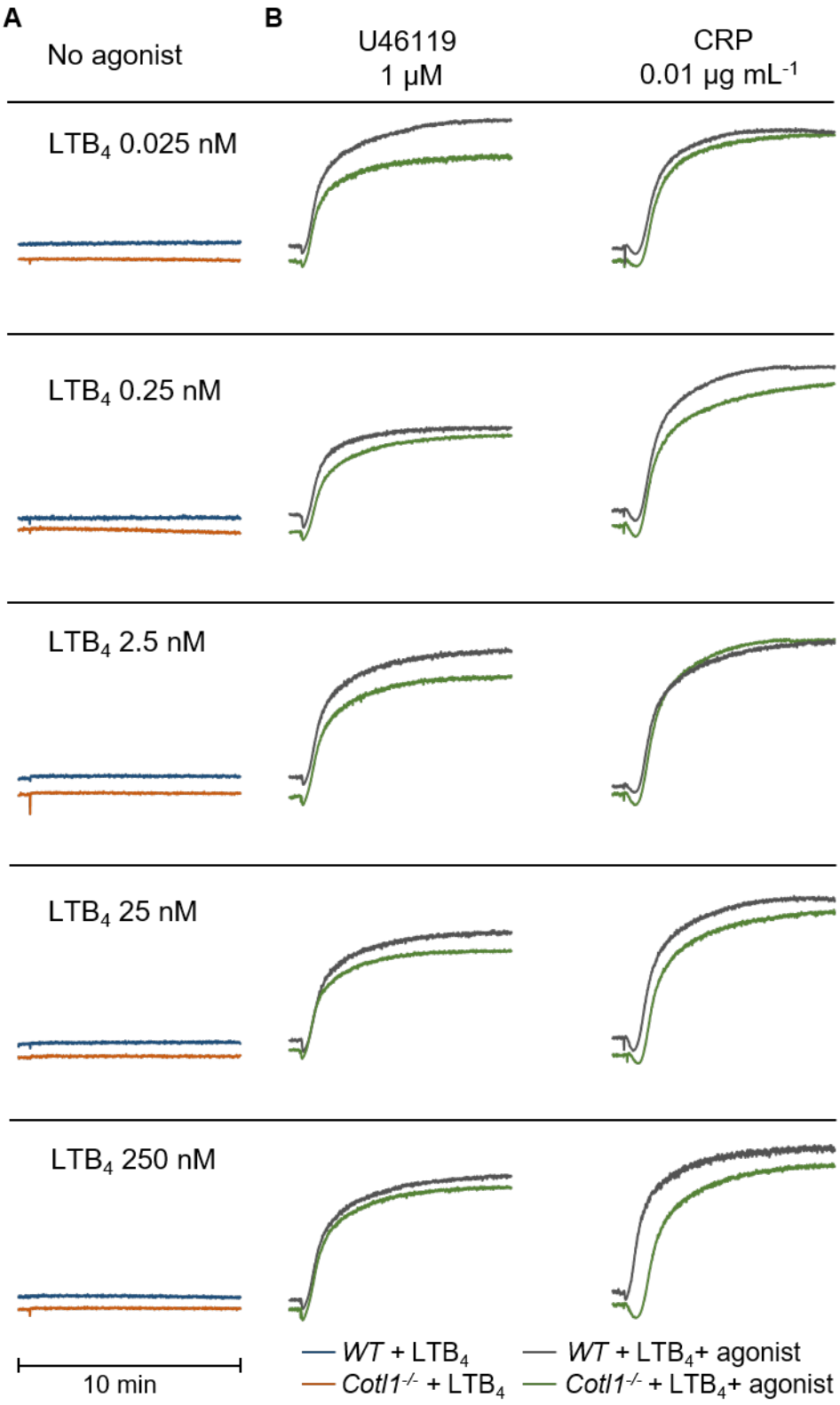

Supplemental Figure 10. LTB_4 treatment does not influence platelet aggregation. (**A, B**) Assessment of platelet aggregation in *WT* and *Cotl1*$^{-/-}$ platelets stimulated with (**A**) 250-0.025 nM LTB_4 or (**B**) co-stimulated with 1 µM U466199 or 0.01 µg mL^{-1} CRP in turbidometric aggregometry.

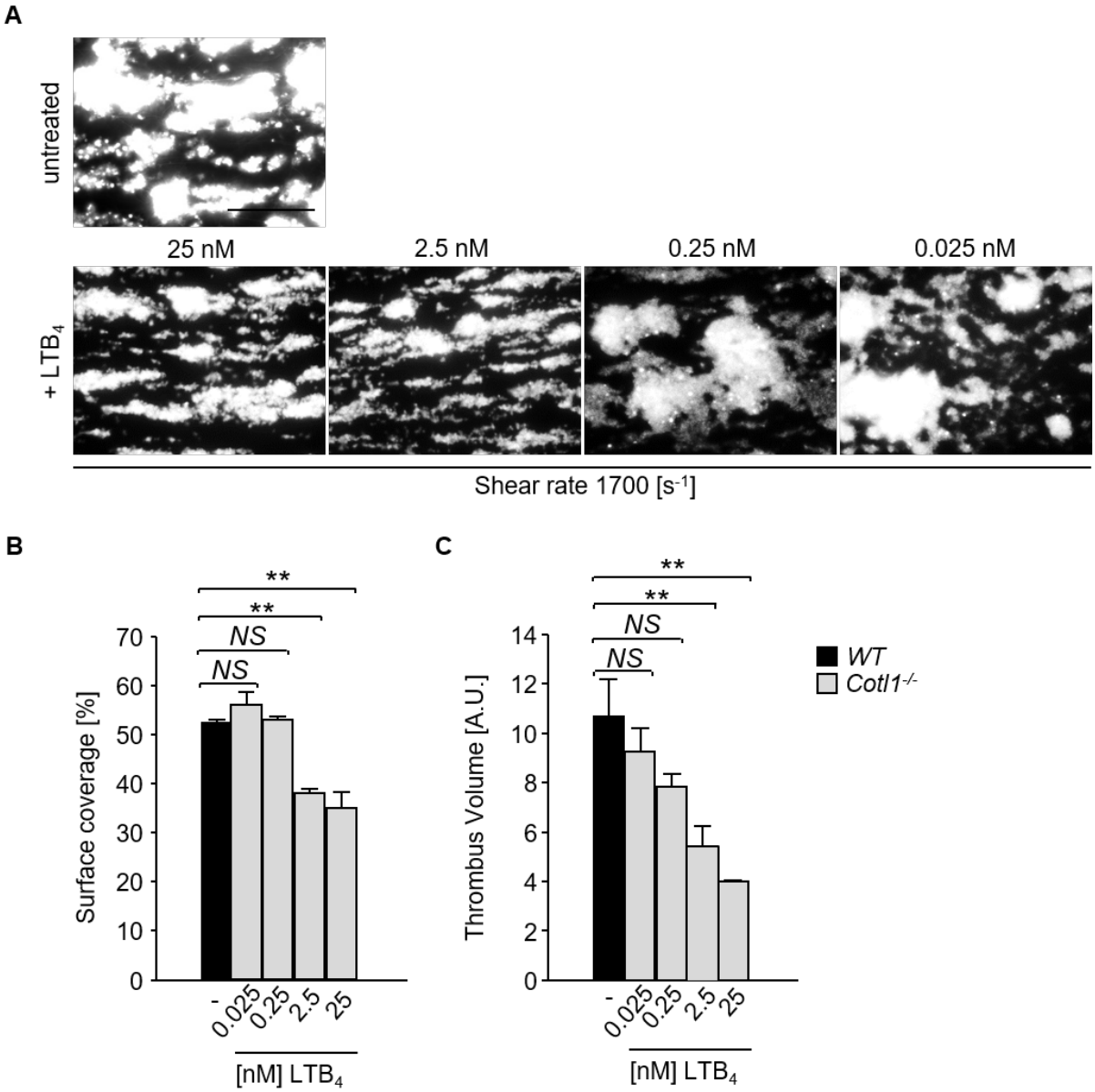

Supplemental Figure 11. Effect of LTB_4 pre-incubation on *WT* blood under flow. (**A-C**) Assessment of platelet adhesion (**A, B**) and aggregate formation (**A, C**) under flow (1700 s^{-1}) on Horm collagen (70 µg mL^{-1}). *WT* samples were either left untreated or were pre-incubated for 5 min with LTB_4 (25- 0.025 nM). Values are mean ± S.D. (n = 12). Scale bar, 50 µm. **P< 0.01. NS, not significant.

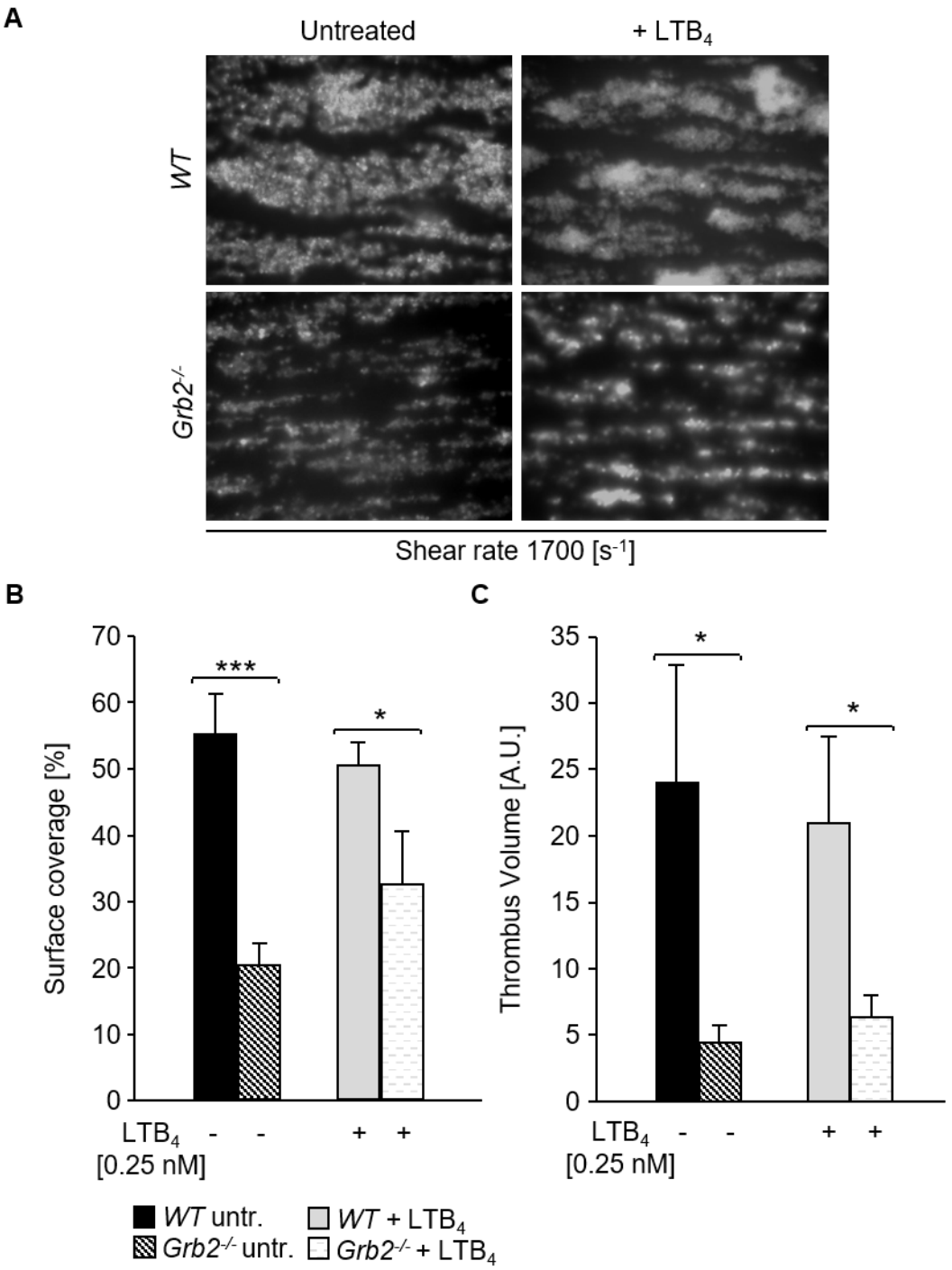

Supplemental Figure 12. Defective shear-dependent thrombus formation in Grb2-deficient mice is not rescued by exogenous addition of leukotriene B_4. (**A-C**) Assessment of platelet adhesion (**A, B**) and aggregate formation (**A, C**) of anticoagulated blood from WT and *Grb2*$^{-/-}$ mice on Horm collagen (70 µg mL^{-1}) under flow (1700 s^{-1}). Samples were either left untreated or were pre-incubated for 5 min with LTB_4 [0.25 nM]. Images are representative of at least 12 mice per group. Values are mean ± S.D. Scale bar, 50 µm. *P< 0.05; ***P< 0.001.

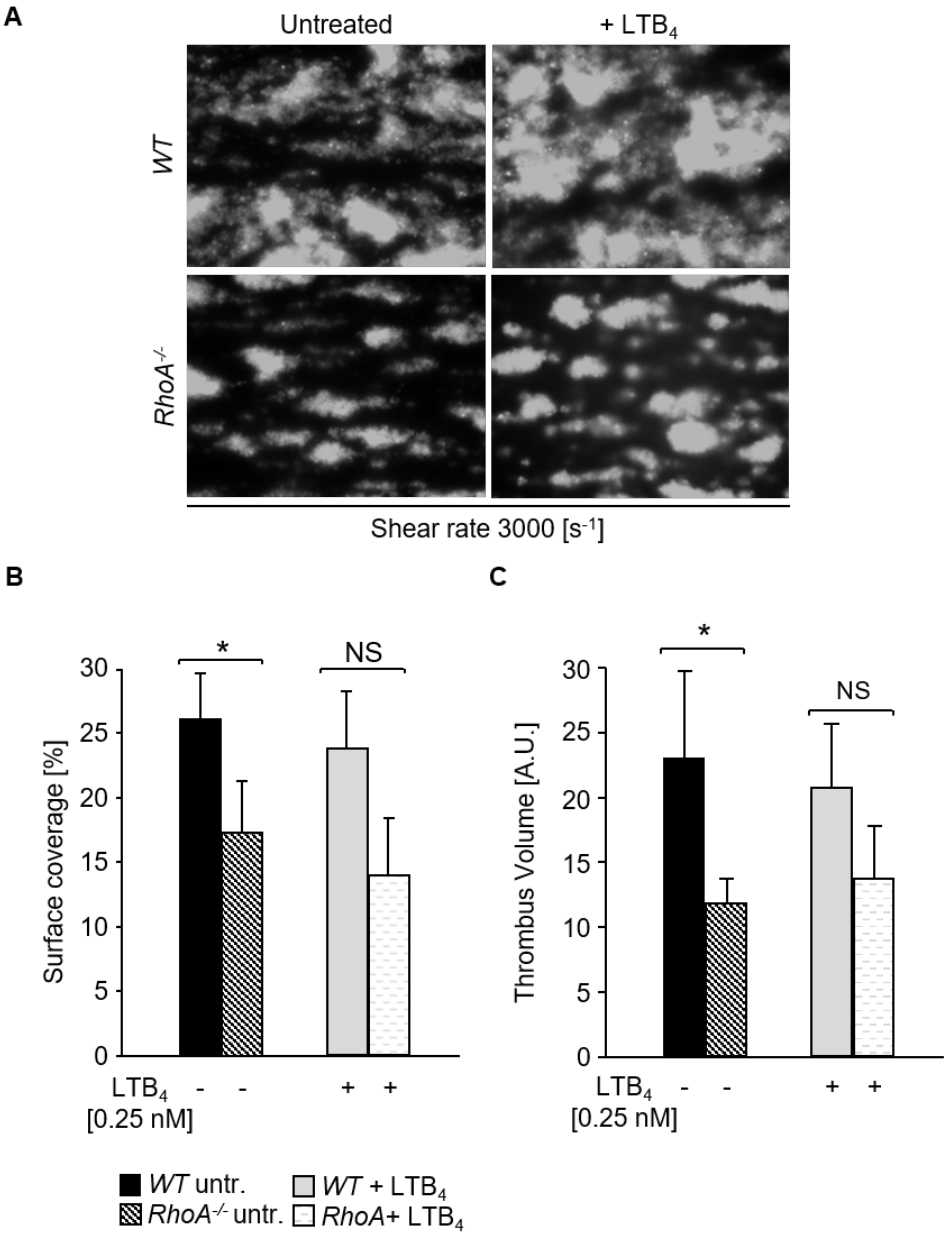

Supplemental Figure 13. Defective shear-dependent thrombus formation in RhoA-deficient mice is not rescued by exogenous addition of leukotriene B_4. (**A-C**) Assessment of platelet adhesion (**A, B**) and aggregate formation (**A, C**) in whole, anticoagulated blood from *WT* and *RhoA*$^{-/-}$ mice on Horm collagen (70 µg mL^{-1}) under flow (1700 s^{-1}). Samples were either left untreated or were pre-incubated for 5 min with LTB_4 [0.25 nM]. Images are representatives of at least 12 mice per group. Values are mean ± S.D. Scale bar, 50 µm. *P< 0.05. NS, not significant.